




K_D determination from time-resolved experiments on live cells with LigandTracer and reconciliation with end-point flow cytometry measurements

Diana Spiegelberg¹ · Jonas Stenberg^{2,3} · Pascale Richalet⁴ · Marc Vanhove^{5,6} 

Received: 30 October 2020 / Revised: 16 June 2021 / Accepted: 1 July 2021 / Published online: 24 July 2021
© The Author(s) 2021

Abstract

Design of next-generation therapeutics comes with new challenges and emulates technology and methods to meet them. Characterizing the binding of either natural ligands or therapeutic proteins to cell-surface receptors, for which relevant recombinant versions may not exist, represents one of these challenges. Here we report the characterization of the interaction of five different antibody therapeutics (Trastuzumab, Rituximab, Panitumumab, Pertuzumab, and Cetuximab) with their cognate target receptors using LigandTracer. The method offers the advantage of being performed on live cells, alleviating the need for a recombinant source of the receptor. Furthermore, time-resolved measurements, in addition to allowing the determination of the affinity of the studied drug to its target, give access to the binding kinetics thereby providing a full characterization of the system. In this study, we also compared time-resolved LigandTracer data with end-point K_D determination from flow cytometry experiments and hypothesize that discrepancies between these two approaches, when they exist, generally come from flow cytometry titration curves being acquired prior to full equilibration of the system. Our data, however, show that knowledge of the kinetics of the interaction allows to reconcile the data obtained by flow cytometry and LigandTracer and demonstrate the complementarity of these two methods.

Keywords LigandTracer · Flow cytometry · Affinity · Binding kinetics · Live-cells measurements

Introduction

Cell surface receptors, including—but not limited to—G-protein-coupled receptors (GPCRs), constitute the most successful class of target proteins for drug discovery research (Cacace et al. 2003). Quantitative measurement of binding affinity is key to searching for and characterizing new

receptor–ligand pairs for drug development. The equilibrium dissociation constant K_D describes the interaction of a drug or ligand L with a receptor R (with $K_D = [L].[R]/[LR]$) and is a critical metric to characterize the binding affinity of ligand–receptor interactions. K_D values are generally either obtained directly from equilibrium titration curves or deduced from either the ratio of the binding kinetics k_{off} (dissociation rate constant) and k_{on} (association rate constant) or from the free energy of binding $\Delta G_{\text{binding}}$ (Hulme and Trevethick 2010; Pan et al. 2013; Pollard 2010).

In recent years, in addition to K_D determination, special emphasis has been given to methodologies that also give access to the binding kinetics, thereby allowing a description of the entire dynamic aspect of ligand–receptor interactions for the prospective design of drugs with improved safety and efficacy profiles, and with better defined binding mechanisms (Andersson et al. 2006; Copeland et al. 2006; Dahl and Akerud 2013; Georgi et al. 2018; Schreiber 2002; Swinney 2008, 2009).

Paralleling the rise of biophysical methods in drug discovery, biophysical instrumentation has also in recent years

✉ Marc Vanhove
m_vanhove@yahoo.com

¹ Department of Surgical Sciences, Uppsala University, 751 85 Uppsala, Sweden

² Ridgeview Instruments AB, Skillsta 4, 740 20 Vänge, Sweden

³ Present Address: A3P Biomedical AB, Vallongatan 1, 752 28 Uppsala, Sweden

⁴ BioRevera, LLC, Scarborough, ME 04074, USA

⁵ Marc Vanhove Consultancy, 4100 Boncelles, Belgium

⁶ Present Address: Oxurion N.V., Gaston Geenslaan 1, 3001 Leuven, Belgium

improved in speed, sensitivity, robustness, and dynamic range, delivering rigorous, reliable, high-definition, and information-rich data. This field is constantly evolving to improve the drug discovery process and to address the new challenges of the next-generation therapeutics (Cariuk et al. 2013; Renaud et al. 2016; Santiveri et al. 2017).

For example, over the past two decades, the need for higher specificity drugs with improved in vivo efficacy and better alignment with physiology has led to a quest for tight binding pairs with sub-nanomolar to picomolar K_D 's (Graff and Wittrup 2003; Rathanaswami et al. 2005; Schreiber 2002; Selzer et al. 2000). As a result, the low concentrations used for these types of assays require sensitive instrumentation. Furthermore, low concentrations and slow dissociation rates result in times to equilibrium that can span days, often exceeding the period of stability of the studied systems and making end-point K_D measurements difficult if not impossible (Andersson et al. 2010; Drake et al. 2018; Vanhove and Vanhove 2018). K_D measurements are also complicated in techniques, such as flow cytometry when $R_0 \gg K_D$ (with R_0 as the total receptor concentration), leading to R_0 -driven interactions, where the value of K_D is easily misinterpreted (Drake and Klakamp 2007; Tamaskovic et al. 2012; Vaish et al. 2020). Pitfalls for proper K_D measurements of tight binders extend to time-resolved techniques even though they do not require equilibrium to be reached: dissociation rates slower than 10^{-5} s^{-1} generally involve several hour-long dissociations requiring stable baselines and rigorous assay settings, often pushing instrumentations to their limits (Barta et al. 2014; Jonsson et al. 2008; Rich and Myszk 2009). The growing trend for tight K_D , therefore, needs to be better supported with methods and technologies that accurately measure these tight interactions (Drake et al. 2018).

Another biophysical challenge faced by the next-generation therapeutics relates to the fact that receptor targets may lose their 3D structure and/or function when isolated. For this reason, the measured K_D values of a therapeutic-target pair can vary widely depending on whether the receptor target is presented on live cells or expressed as a recombinant protein (Cariuk et al. 2013; Drake et al. 2018; Nilvebrant et al. 2012; Rathanaswami et al. 2008). The discrepancy of K_D values can also extend to the same ligand–receptor pair among different cell lines, highlighting cell-dependent receptor landscapes and receptor subunit pairing (Barta et al. 2014; Bjorkelund et al. 2011). As a result, technologies and methods applicable to live cells strengthen the physiological relevance of biophysical measurements and are, for that reason, gaining in popularity (Bondza et al. 2017; Drake et al. 2018; Rathanaswami et al. 2008; Renaud et al. 2016; Wood et al. 2004).

LigandTracer is a relatively new technology that allows real-time monitoring of ligand–receptor interaction on live cells (Bjorke and Andersson 2006; Bondza et al. 2017). Similar to other time-resolved techniques, where one molecular partner is immobilized while the other is added to the medium, the resulting time-traces represent the number of ligand–receptor (LR) complexes forming or dissociating over time and thus contain the kinetic information characterizing the studied molecular interaction (Canziani et al. 2004; Dubois et al. 2013). Binding kinetics are extracted from global fitting of the curves, and the value of K_D can be calculated from the ratio of the binding kinetics without the need to reach equilibrium. The use of live cells exposing native receptors circumvents the need for recombinant targets. Furthermore, LR complex dissociation can be monitored for several hours making it suitable for the characterization of slowly dissociating drugs. Here we report LigandTracer data for five tight therapeutic antibody–receptor pairs to illustrate the potential of the technology.

Furthermore, we compare LigandTracer kinetic data with traditional endpoint-based flow cytometry data. Flow cytometry-based K_D measurements also use live cells and involve the titration of a fixed number of cells with various concentrations of a fluorescent ligand for a specific time. The resulting curve, representing the amount of LR complex formed as a function of the ligand concentration, is typically analyzed based on a 1:1 equilibrium model to extract the K_D value (Drake and Klakamp 2007; Tamaskovic et al. 2012; Vaish et al. 2020). This end-point technique relies on the hypothesis that the incubation time used in the experiment is sufficiently long to reach equilibrium. Our kinetic data suggest that this prerequisite can be difficult to achieve in practice. Instead, we propose a general methodology combining LigandTracer and flow cytometry measurements, the two methods complementing each other to provide the best and most accurate description of the studied system.

Materials and methods

Cell culture

Cell lines (all from ATCC) were cultured in a humidified incubator at 37 °C with 5% CO₂. SKBR3 cells expressing HER2 were grown in ATCC-formulated McCoy's 5a Medium Modified (ATCC, Manassas, VA), supplemented with 10% FBS (Millipore-Sigma, Burlington, MA). HER2-expressing ovarian carcinoma SKOV3 cell lines were cultured in Ham's F10 medium (Biochrom AG, Berlin, DE) supplemented with 10% FBS (Millipore-Sigma, Burlington, MA), 1% L-glutamine, and 1% penicillin–streptomycin (Biochrom AG, Berlin, DE). Daudi cells were cultured in RPMI

1640 cell culture medium (Biochrom AG, Berlin, DE) with the same supplements as above.

Antibodies and labeling

Trastuzumab (Apoteket, Sweden), Pertuzumab (Omnitarg™; Genentech, South San Francisco, CA), Rituximab (Apoteket, Sweden), Cetuximab (Apoteket, Sweden) were fluorescently labeled for LigandTracer and/or flow cytometry experiments. Trastuzumab was labeled with Mix-n-Stain™ CF™ 488A and Mix-n-Stain™ CF™ 647 Antibody Labeling Kits (Millipore-Sigma, Burlington, MA) for LigandTracer and flow cytometry experiments, respectively, according to the manufacturer's recommendations. Rituximab, Pertuzumab, and Cetuximab were labeled with fluorescein isothiocyanate (FITC) (Millipore-Sigma, Burlington, MA) for flow cytometry experiments. FITC was dissolved at 1 µg/µL in DMSO. Antibodies in PBS were diluted in twice the volume of borate buffer pH 9, and 100 ng of FITC was added per µg of antibody. The samples were incubated at 37 °C for 90 min. Labeled proteins were purified by buffer exchange on NAP-5 columns (GE Healthcare) and stored in aliquots at –20 °C prior to use (Bondza et al. 2017).

LigandTracer

SKBR3 cells were lifted with Accutase® (Millipore-Sigma, Burlington, MA), counted, and re-suspended at a density of 3.3×10^5 cells/mL in full medium. Three milliliters of the cell suspension were seeded to tilted cell culture treated Petri dishes (Nunc #150350, ThermoFisher, Waltham, MA) and allowed to adhere to the plastic for 4 h at 37 °C after which the medium was replaced by 12 mL of fresh medium and the plates were incubated overnight horizontally. LigandTracer® experiments were conducted 2–3 days after seeding.

Binding of Trastuzumab-A488 to SKBR3 cells was measured with LigandTracer Green (Ridgeview Instruments AB, Uppsala, Sweden) using a blue (488 nm)–green (535 nm) detector. Experiments were performed essentially as previously described (Bondza et al. 2017). In short, a Petri dish with adherent cells in a confined area and 3 mL of fresh culture medium with 0.1% sodium azide (Millipore-Sigma) to prevent internalization was placed on an inclined, rotating support in the instrument. After 30 min of baseline measurement, two increasing concentrations of a fluorescently labeled antibody were added sequentially and signals from cell target and background reference areas were recorded over time. Each sample was incubated for 2–5 h until sufficient curvature was obtained. Antibody dissociation from target was measured for 9 h after replacement of the incubation solution with fresh medium either in the absence or

in the presence of an excess of unlabeled antibody. Kinetic traces were analyzed with TraceDrawer (Ridgeview Instruments AB, Uppsala, Sweden) using either a standard one-to-one binding model (referred to as “OneToOne model” in TraceDrawer, and essentially similar to Eq. 7 below) or, for situations where the number of ligand molecules is close to the number of receptors, a binding model corrected for ligand depletion (referred to as “OneToOneDepletionCorrected model” in TraceDrawer, and essentially similar to Eq. 2 below).

Experimental conditions to obtain LigandTracer kinetic data for Rituximab, Pertuzumab, Cetuximab, and Panitumumab were described elsewhere (Bondza et al. 2017; Barta et al. 2014).

Flow cytometry

SKBR3 cells were re-suspended in 10 mL of full medium after harvest, counted, and allowed to recover for 1 h at 37 °C. Although it is unclear from the literature whether Trastuzumab remains at the cell surface or internalizes (Ram et al. 2014), cells were spun down and re-suspended at 1×10^6 cells/mL at room temperature in full medium containing 0.1% sodium azide to prevent internalization. A total of 2.0×10^5 cells in 200 µL were added per well of round bottom polypropylene 96-well plates (USA scientific). Plates were spun down at 4000 rpm for 4 min and flipped down vigorously once. Twenty-one concentrations of Trastuzumab-CF 647 ranging from 0.02 to 150 nM in full medium containing 0.1% sodium azide were added per well, in triplicate, for 3.5 h at room temperature and under gentle rocking. Plates were then spun down and fresh medium was added. The gate on live cells population was taken from a control cell well (without any antibody) and Guava® easy-Cyte benchtop instrument (Millipore-Sigma) was set up to acquire 5000 events.

SKOV3 cells were re-suspended in 10 mL full of medium after harvest, counted, and allowed to recover for 1 h at 37 °C in full medium. Cells were then spun down (4000 rpm, 4 min) and re-suspended at a concentration of 1×10^6 cells/mL. Cells were added to an antibody titration series of 0.07–100 nM and incubated in the dark for 2 h at room temperature under gentle rocking followed by analysis using a BD LSRII SORP (Becton Dickinson Biosciences, San Jose, USA) flow cytometer. The gate on live cells population was taken from a control cell well (without any antibody) and 10,000 events were collected.

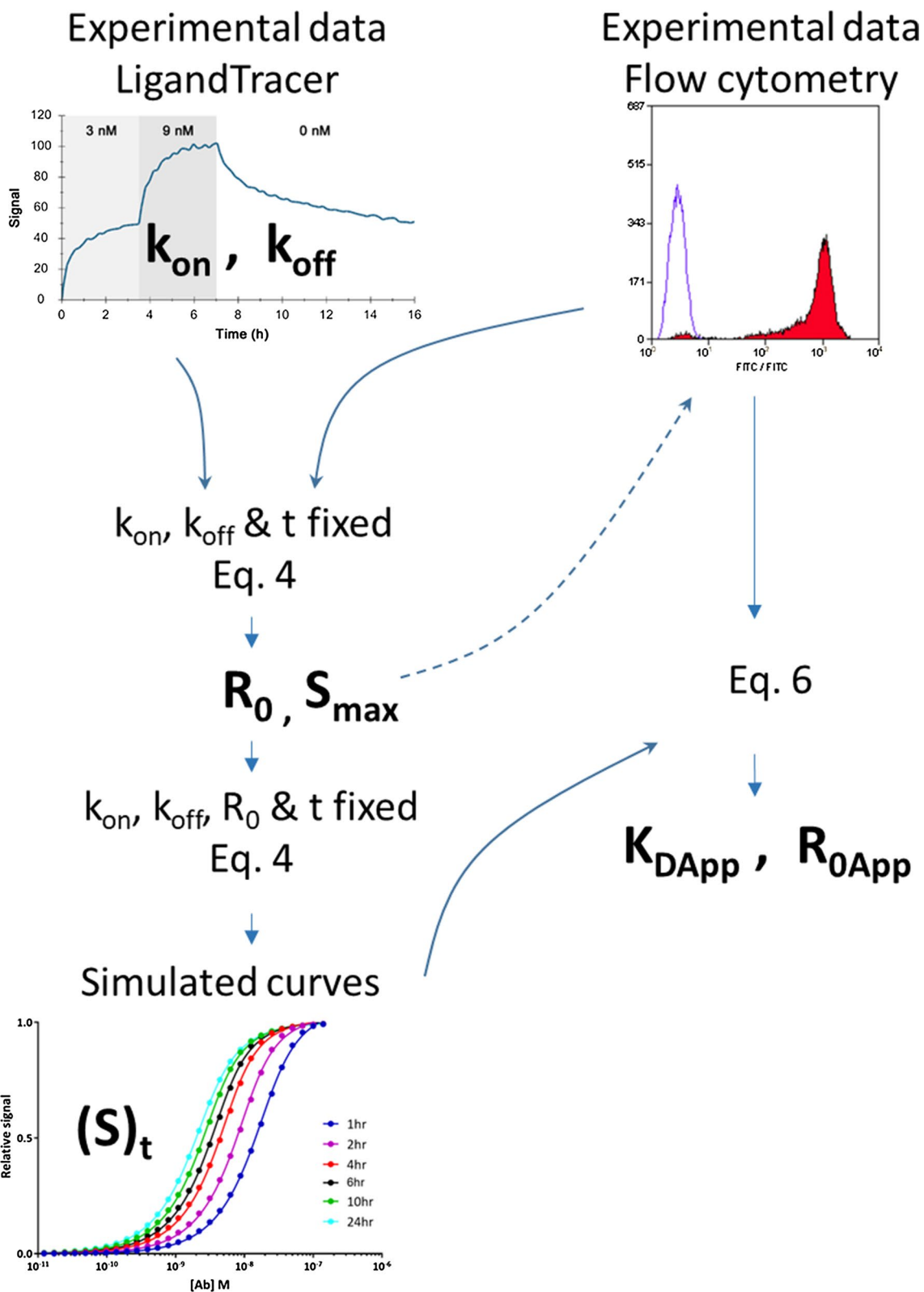


Fig. 1 Overview of data analysis workflow. Bold characters indicate calculated variable values. Experimental LigandTracer data were used to calculate the kinetic constants k_{on} and k_{off} . Experimental flow cytometry data were then fitted to Eq. 4 with binding kinetics obtained from LigandTracer and incubation time as constants, giving access to the receptor concentration term R_0 . Binding kinetics and R_0 values were used in Eq. 4 to simulate flow cytometry data at various incubation times, allowing a visual assessment of the progress of the reaction towards equilibrium. Both simulated and experimental flow cytometry data were then analyzed with Eq. 6 to calculate the apparent equilibrium dissociation constant (K_{DApp}) and apparent receptor concentration (R_{0App})

Equations used

In its simplest form, binding of a ligand L to its cognate receptor R can be written as Eq. 1, where k_{on} and k_{off} are the association and the dissociation rate constants, respectively:



The differential equation describing $[LR]$ versus time can be expressed as Eq. 2, where L_0 and R_0 are the total concentration of L and R , respectively, and $[LR]_t$ is the concentration of the complex LR at time t :

$$\frac{\partial [LR]_t}{\partial t} = k_{on} \cdot (R_0 - [LR]_t) \cdot (L_0 - [LR]_t) - k_{off} \cdot [LR]_t. \tag{2}$$

The integrated form of Eq. 2 was recently proposed by Vanhove and Vanhove (2018) in the form of Eq. 3, which allows to express $[LR]_t$ as a function of k_{on} , k_{off} , R_0 , L_0 , and t :

$$[LR]_t = \frac{a \cdot (1 - c) - b \cdot (1 + c)}{2 \cdot k_{on} \cdot (1 - c)} \tag{3}$$

where $a = k_{on} \cdot (L_0 + R_0) + k_{off}$; $b = \sqrt{a^2 - 4 \cdot k_{on}^2 \cdot L_0 \cdot R_0}$; $c = \left(\frac{a-b}{a+b}\right) \cdot e^{-b \cdot t}$.

The experimental signal (S_t), whether in flow cytometry or LigandTracer experiments, is directly proportional to the concentration of complex LR and can thus be expressed as Eq. 4, where S_{max} is the maximum signal, i.e., the signal at saturating ligand concentrations, and where $[LR]_t$ is given by Eq. 3:

$$(S)_t = S_{max} \cdot \frac{[LR]_t}{R_0}. \tag{4}$$

Equation 4 allows the analysis of pre-equilibrium titration curves. Of note, Eq. 3 is derived without any mathematical simplification and is thus not limited to pseudo first-order reactions, where $L_0 \gg R_0$ (Vanhove and Vanhove 2018).

At $t = \infty$, $c = 0$ and Eqs. 3 and 4 can be simplified into Eqs. 5 and 6, respectively, where $[LR]_e$ is the concentration of complex LR at equilibrium (Vanhove and Vanhove 2018):

$$[LR]_e = \left(\frac{L_0 + R_0 + K_D}{2}\right) - \sqrt{\left(\frac{L_0 + R_0 + K_D}{2}\right)^2 - L_0 \cdot R_0} \tag{5}$$

$$(S)_t = S_{max} \times \frac{[LR]_e}{R_0}. \tag{6}$$

Finally, when $L_0 \gg R_0$, Eq. 2 can be simplified into Eq. 7 which, following a reasoning similar as above, leads to Eq. 8 (Morton et al. 1995):

$$\frac{\partial [LR]_t}{\partial t} = k_{on} \cdot (R_0 - [LR]_t) \cdot L_0 - k_{off} \cdot [LR]_t \tag{7}$$

$$(S)_t = S_{max} \cdot \left(\frac{L_0}{L_0 + K_D}\right) \cdot \left(1 - e^{-(k_{on} \cdot L_0 + k_{off}) \cdot t}\right). \tag{8}$$

Data analysis

An overview of the data analysis workflow is shown in Fig. 1.

LigandTracer data were analyzed with TraceDrawer to compute k_{on} and k_{off} values. When shown, the U value was used to measure the precision of the fits and defines how much a given kinetic parameter can vary before the results show significant changes. The lower the U value, the better the fit. A U value > 15 for example indicates that the binding kinetics can be altered by 15% or more without significantly affecting the fitted curve. The U value takes parameter dependency into account and is, therefore, a safer quality value than χ^2 or T values (Onell and Andersson 2005).

Experimental flow cytometry data were first fitted with Eq. 4 with the help of the GraphPad Prism software (GraphPad Software Inc., La Jolla, CA) using the k_{on} and k_{off} values obtained from LigandTracer experiments and fixing the term t to the actual incubation time, which allowed the determination the parameters R_0 and S_{max} . The number of receptors per cell was then calculated from the Avogadro number and the number of cells used in the experiment. For A431 cells, since experimental flow cytometry data for Panitumumab–EGFR binding were not generated, the value of R_0 was taken from Barta et al. (2011) and fixed to 2×10^6 receptors/cell. Equation 4 was then used to simulate flow cytometry curves at different incubation time based on the value of S_{max} , R_0 , k_{on} , and k_{off} obtained as described above.

Table 1 Binding kinetics and K_D values from LigandTracer measurements for the indicated antibody-receptor pairs, and receptor concentrations (R_0) computed from flow cytometry data

Systems studied	Binding kinetics from LigandTracer				Flow cytometry, Eq. 6		Receptor density (million per cell)					
	Cell type	k_{on} ($M^{-1} s^{-1}$)	k_{off} (s^{-1})	K_D (M)	Reference	R_0 (M)	R_0/K_D	R_0/K_D	R_{0App} (M)	This paper	Literature	Reference
Rituximab-CD20	Daudi	1.4×10^4	1.3×10^{-5}	9.3×10^{-10}	Bondza et al. (2017)	5.0×10^{-9}	5.3	3.9×10^{-9}	2.2×10^{-8}	3	0.13–0.21	Bondza et al. (2020)
Trastuzumab-HER2	SKBR3	2.4×10^4	5.4×10^{-6}	2.2×10^{-10}	This paper	9.9×10^{-9}	45	1.7×10^{-9}	6.7×10^{-9}	5.9	5–6	Barta et al. (2011)
Pertuzumab-HER2	SKOV3	5.5×10^4	7.0×10^{-6}	1.3×10^{-10}	Bondza et al. (2017)	1.0×10^{-8}	79	4.1×10^{-10}	9.5×10^{-9}	10	5–6	Barta et al. (2011)
Panitumumab-EGFR	A431	6.3×10^4	1.6×10^{-6}	2.5×10^{-11}	Barta et al. (2014)	3.3×10^{-9a}	130	NA	NA	NA	2–5	Barta et al. (2011)
Cetuximab-EGFR	SKOV3	9.0×10^5	1.2×10^{-6}	1.3×10^{-12}	Bondza et al. (2017)	2.2×10^{-9}	1700	8.4×10^{-11}	2.3×10^{-9}	1	0.1–0.3	Barta et al. (2011)

The incubation times for flow cytometry measurements were 1 h for Rituximab and Cetuximab, 2 h for Pertuzumab and Trastuzumab, and 3.5 h for Trastuzumab. Receptor concentrations were also converted to receptor density on cells and compared to published data. Finally, K_{DApp} and R_{0App} values obtained by analysis of flow cytometry data assuming equilibrium are also presented

NA data not available

^aExcept for Panitumumab-EGFR, for which the R_0 value was obtained from Barta et al. (2011)

In a second stage, flow cytometry data (normalized based on S_{max} to facilitate visual comparison) were fitted to Eq. 6 (using the Graphpad Prism software) without constraints. Since it was a priori not known whether the system was fully at equilibrium when the data were acquired, fitting with Eq. 6 yielded only apparent values for K_D and R_0 which will be referred to here as and K_{DApp} and R_{0App} .

Finally, time to equilibrium for a given ligand concentration was calculated from the ratio of Eqs. 3 and 5, the $[LR]/[LR]_e$ ratio representing the degree of completion of the reaction at a given time. A ratio of 1 indicates that the equilibrium has been reached.

Results

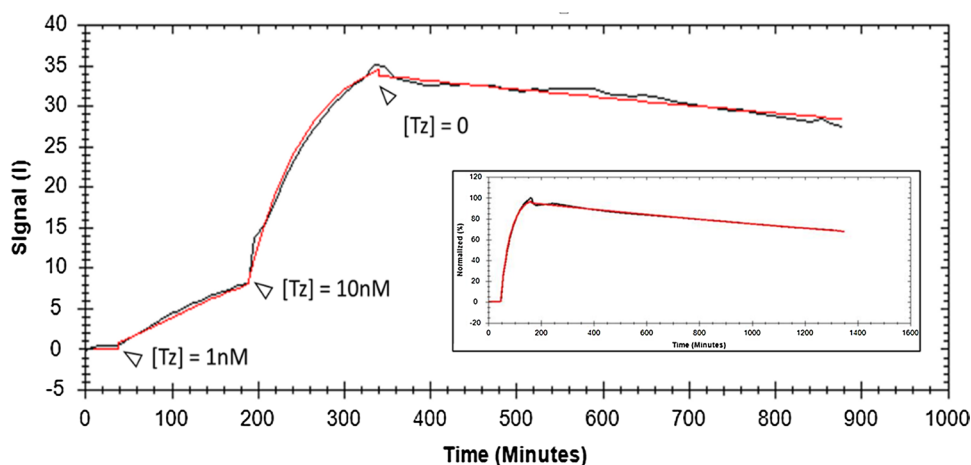
Binding kinetics with LigandTracer

Except for Trastuzumab binding to HER2 on SKBR3 cells, binding kinetics have been reported elsewhere (see data with respective references in Table 1). LigandTracer data for Trastuzumab are shown in Fig. 2. The kinetic traces could be accurately analyzed with a standard 1:1 binding model with the help of the TraceDrawer software with low χ^2 and U values of 0.36 and 1.90, respectively, leading to k_{on} , k_{off} , and calculated K_D values of $2.4 \times 10^4 M^{-1} s^{-1}$, $5.4 \times 10^{-6} s^{-1}$, and $2.2 \times 10^{-10} M$, respectively. Data analysis using a binding model corrected for ligand depletion yielded identical parameters. To be noted, and despite a dissociation rate $< 10^{-5} s^{-1}$, the dissociation phase showed a decrease of 14%, allowing robust k_{off} estimation (the experiment was repeated independently twice resulting in identical K_D values and binding kinetics parameters within 2% standard deviation—not shown). In addition, worth noting, following the dissociation of Trastuzumab-A488 from SKBR3 cells in the presence of an excess of unlabeled antibody (insert in Fig. 2) provided a k_{off} value of $4.7 \times 10^{-6} s^{-1}$ in excellent agreement with the value reported above, which demonstrates that rebinding of the antibody during the dissociation phase can be neglected.

Flow cytometry

Experimental flow cytometry data for binding of Rituximab to CD20-expressing Daudi cells (incubation time 1 h), Trastuzumab and Pertuzumab to HER2-expressing SKOV3 cells (incubation time 3.5 and 2 h, respectively), and Cetuximab to EGFR-expressing SKOV3 cells (incubation time 2 h) are shown in Fig. 3. Worth mentioning, these incubation times, although selected arbitrarily, correspond to incubation times generally used for this kind of experiment, since longer incubation times are often associated

Fig. 2 Time course (signal intensity vs. time) for binding of Trastuzumab–A488 (Tz) to SKBR3 cells. Two antibody concentrations of 1 and 10 nM were added sequentially for 150 and 200 min, respectively, and dissociation was followed for 9 h. The fitted curve for a 1:1 binding model is shown in red. Calculated values and fitting parameters are reported in the table below the curve. The insert shows the dissociation of Trastuzumab–A488 in the presence of 10 nM unlabeled antibody ($[Tz] = 10$ nM for the association phase)



k_{on} ($M^{-1}s^{-1}$)	k_{off} (s^{-1})	K_D (M)	S_{max}	χ^2	U
2.4×10^4	5.4×10^{-6}	2.2×10^{-10}	37.6	0.36	1.9

with cell viability issues. For example, Freeman et al. (2012) performed flow cytometry titration experiments with Panitumumab on EGFR-expressing A431 cells with 1 h incubation time. We did not, however, assume that the different systems were necessarily at equilibrium at the indicated incubation times. Data analysis using Eq. 6 was thus not appropriate. Instead, we chose to fit the flow cytometry traces to Eq. 4, fixing the kinetic parameters k_{on} and k_{off} to the values obtained from LigandTracer experiments which allowed to extract the value of the receptor concentration (R_0) for each system and cell type, from which the number of receptor molecules per cell was calculated. These values are reported in Table 1 and are consistent with published data for at least HER2-expressing SKBR3 and SKOV3 cells. For EGFR-expressing A431 cells, in the absence of flow cytometry data with Panitumumab, R_0 was fixed to a value corresponding 2×10^6 receptors/cell based on Barta et al (2011).

Equation 4 was then used to generate theoretical flow cytometry traces for the different systems and for various times of incubation (Fig. 3). From this, it is immediately evident for all studied systems except Cetuximab–EGFR that full equilibration requires incubation times significantly longer than 1 h, the Rituximab–CD20, Trastuzumab–HER2, and Panitumumab–EGFR systems being the slowest to equilibrate.

Flow cytometry experiments performed with the objective of determining the affinity of antibodies to cell surface receptors are generally analyzed using Eq. 6 assuming that the system is at equilibrium. The extent to which the computed parameters R_0 and K_D deviate from their exact value when that latter hypothesis is not fulfilled can be appreciated

by fitting either actual flow cytometry data sets acquired prior to equilibrium or theoretical simulated flow cytometry curves generated for different incubation times with Eq. 6 (Fig. 4A, B). This analysis reveals that R_0 and K_D values computed prior to full equilibration (R_{0App} and K_{DApp}) differ to a great extent from the intrinsic R_0 and K_D values, even when visual observation of the curves suggests that the system is almost at equilibrium (see data for Cetuximab).

Altogether, these observations highlight the benefit of combining LigandTracer-based kinetic determination with flow cytometry experiments, especially for slowly equilibrating systems which may require incubation times far exceeding the time during which the reagents are stable to reach the equilibrium.

Time to equilibrium

The time for a system to reach 97% of the final equilibrium has been described by Eq. 9 (Andersson et al. 2010; Hulme and Trevethick 2010):

$$t_{eq} = \frac{5 \cdot \ln 2}{(k_{on} \cdot L + k_{off})} \quad (9)$$

The above expression, however, assumes that the considered reaction obeys pseudo-first-order kinetics, which is true only if $L_0 \gg R_0$. To assess the degree of completeness of the reaction, we, therefore, propose to use the ratio of $[LR]_t$ versus $[LR]_e$ as obtained from Eqs. 3 and 5. The closer to 0, the further away the system is from equilibrium. Conversely, a ratio of 1 indicates that the system has reached equilibrium.

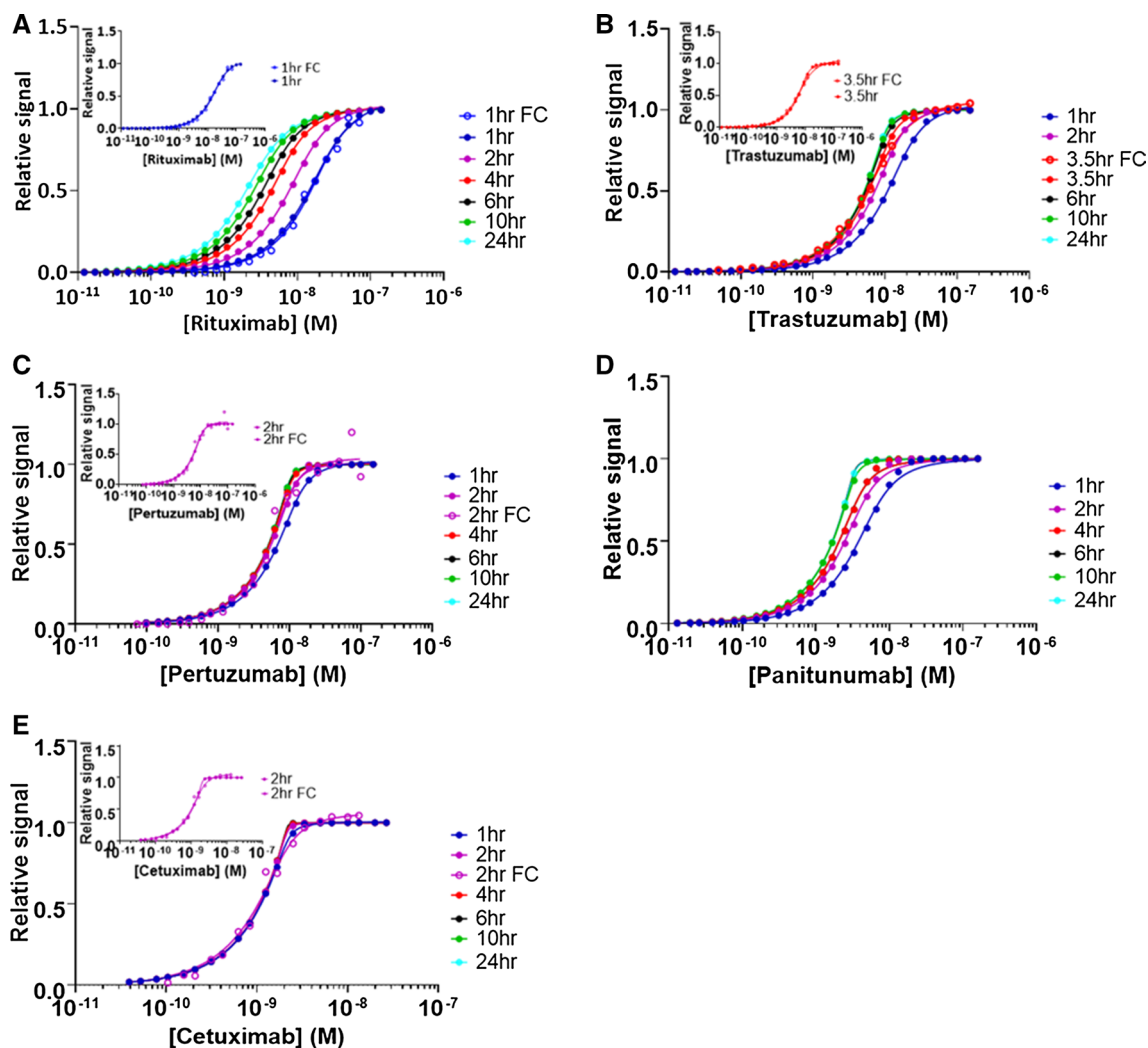


Fig. 3 Comparison of normalized experimental flow cytometry (FC) data recorded at the indicated incubation time (average from duplicate or triplicate measurements) with flow cytometry data simulated for various incubation times with Eq. 4. **A** Rituximab–CD20 on Daudi cells, experimental flow cytometry incubation time 1 h with 10^6 cells/mL; **B** Trastuzumab–HER2 on SKOV3 cells, experimental flow cytometry incubation time 3.5 h with 10^6 cells/mL; **C** Pertuzumab–

HER2 on SKOV3 cells, experimental flow cytometry incubation time 2 h with 6×10^5 cells/mL; **D** Panitumumab–EGFR on A431 cells, only simulated flow cytometry data assuming 10^6 cells/mL; **E** Cetuximab–EGFR on SKOV3 cells, experimental flow cytometry incubation time 2 h with 1.33×10^6 cells/mL. The thumbnails in **A**, **B**, **C**, and **E** represent the experimental flow cytometry data together with the data simulated at the same incubation time

Figure 5 represents plots of $[LR]_t/[LR]_e$ versus L_0 for various incubation times for all the systems studied here, offering a visual assessment of time to equilibrium for all molecular pairs under their specific experimental settings. For example, the fast-equilibrating Cetuximab–EGFR and Pertuzumab–HER2 systems requires 1–3 h and 6–10 h for full equilibration, respectively, while the other systems have reached equilibrium for all ligand concentrations only after ~ 24 h. It can also be appreciated that all considered systems are predicted to be at equilibrium for the highest ligand concentrations even for the shortest incubation time considered here, i.e., 1 h. Conversely, the time

to equilibrium is longer for lower ligand concentrations. Interestingly, though, the value of $[LR]_t/[LR]_e$ reaches for all systems a minimum for L_0 values roughly around 10^{-9} – 10^{-8} M as shown as a dip in the curves. Although counter-intuitive, this indicates that the ligand concentration that requires the longest time to reach equilibrium is not necessarily the lowest concentration used in an experimental setting. A formal mathematical demonstration of this observation would require calculating the L_0 value for which the derivative of the $[LR]_t/[LR]_e$ expression (with $[LR]_t$ and $[LR]_e$ as per Eqs. 3, 5) is equal to zero, which is complex and far beyond the scope of this work. Instead,

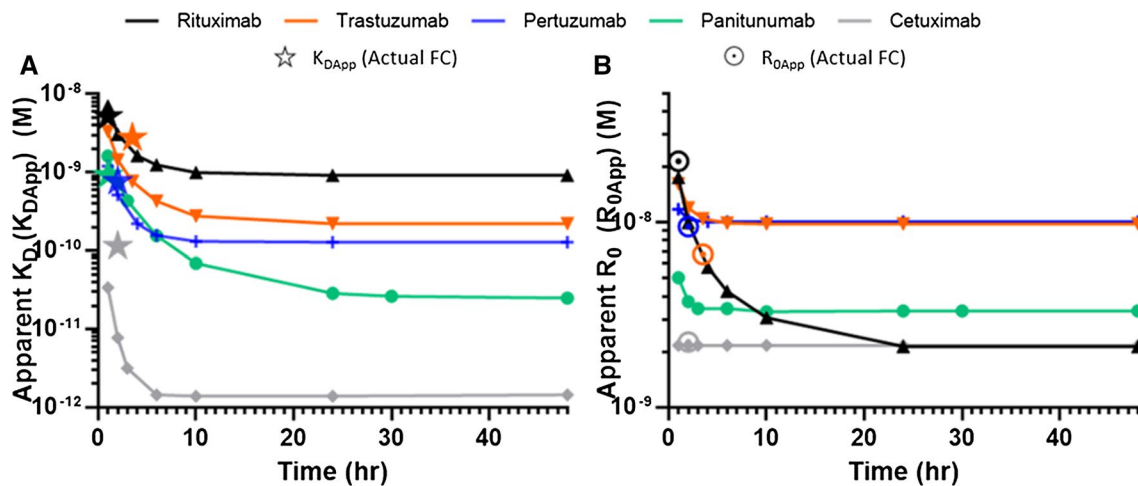


Fig. 4 Experimental flow cytometry (FC) data as well as flow cytometry data simulated for various incubation times based on Eq. 4 were fitted with Eq. 6 to compute apparent equilibrium dissociation constants (K_{DApp}) and apparent receptor concentrations (R_{0App}). **A** K_{DApp}

values. The stars correspond to K_{DApp} values obtained from the experimental flow cytometry data sets. **B** R_{0App} values. The dotted disks correspond R_{0App} values obtained from the experimental flow cytometry data sets

the numerical methodology proposed here allows to easily assess the time needed to reach the equilibrium for any pre-defined experimental conditions.

Discussion

LigandTracer information on kinetic constants to strengthen flow cytometry data

From Eq. 1, which describes the interaction between a ligand L and its receptor R , the rate of LR complex formation over time can be expressed without simplification as Eq. 2 or, assuming that $L_0 \gg R_0$, as Eq. 7. These are differential equations, which is the form usually used by software to globally analyze time-resolved binding data through numerical integration. Equation 2 (or variations thereof) is useful to analyze data generated under conditions where $L_0 \sim R_0$, and TraceDrawer is, to our knowledge, the only commercially available software offering it as an option.

Equation 4, or its simplified version (Eq. 8), are better suited to be used in software's such as Excel for data simulation or GraphPad Prism for non-linear regression analysis. Eq. 4, derived from Eq. 3, and which can be used to describe or analyze pre-equilibrium titration curves, is, however, complex and may not be ideally suited to analyze only one set of flow cytometry data obtained for a specific incubation time. We, therefore, propose to use the kinetic parameters k_{on} and k_{off} obtained from LigandTracer experiments as constants to “stabilize” the equation and allow robust determination of the receptor concentration R_0 , as exemplified in this manuscript.

Fitting of flow cytometry data with Eq. 6 is only recommended if the system has reached full equilibrium. When that condition is not perfectly fulfilled, data analysis with Eq. 6 can return R_0 and K_D values that can deviate substantially from the true values of these parameters depending not only on the degree of completion of the reaction but also, to a certain extent, on the relationship between R_0 and K_D (Vaish et al. 2020).

The systems studied here can be sorted into three groups based on their respective R_0/K_D ratio (Table 1), namely, (1) Rituximab–CD20 ($R_0 \sim K_D$); (2) Trastuzumab–HER2, Pertuzumab–HER2 and Panitumumab–EGFR ($R_0 > K_D$); and (3) Cetuximab–EGFR ($R_0 \gg K_D$). As discussed elsewhere (Drake et al. 2018; Drake and Klakamp 2007; Tamaskovic et al. 2012; Vanhove and Vanhove 2018), experimental data obtained under conditions where $R_0 \sim K_D$ allows the determination of both parameters, while only R_0 can be robustly determined when $R_0 \gg K_D$. This also applies to analysis of pre-equilibrium titration curves with Eq. 4 (Vanhove and Vanhove 2018). Therefore, determination of K_D values from flow cytometry data without the support of information on the kinetics of the interaction such as provided by LigandTracer would have been challenging or impossible for all studied systems except Rituximab–CD20, and this regardless of whether the data would have been generated under conditions of pre-equilibrium and analyzed with Eq. 4 or under conditions of full equilibrium and analyzed with Eq. 6.

When conducting flow cytometry experiments with the objective of analyzing a given system at equilibrium, it is common practice to run the experiment at two (or more) incubation times and to consider in practice that the system has reached its equilibrium if the different data sets,

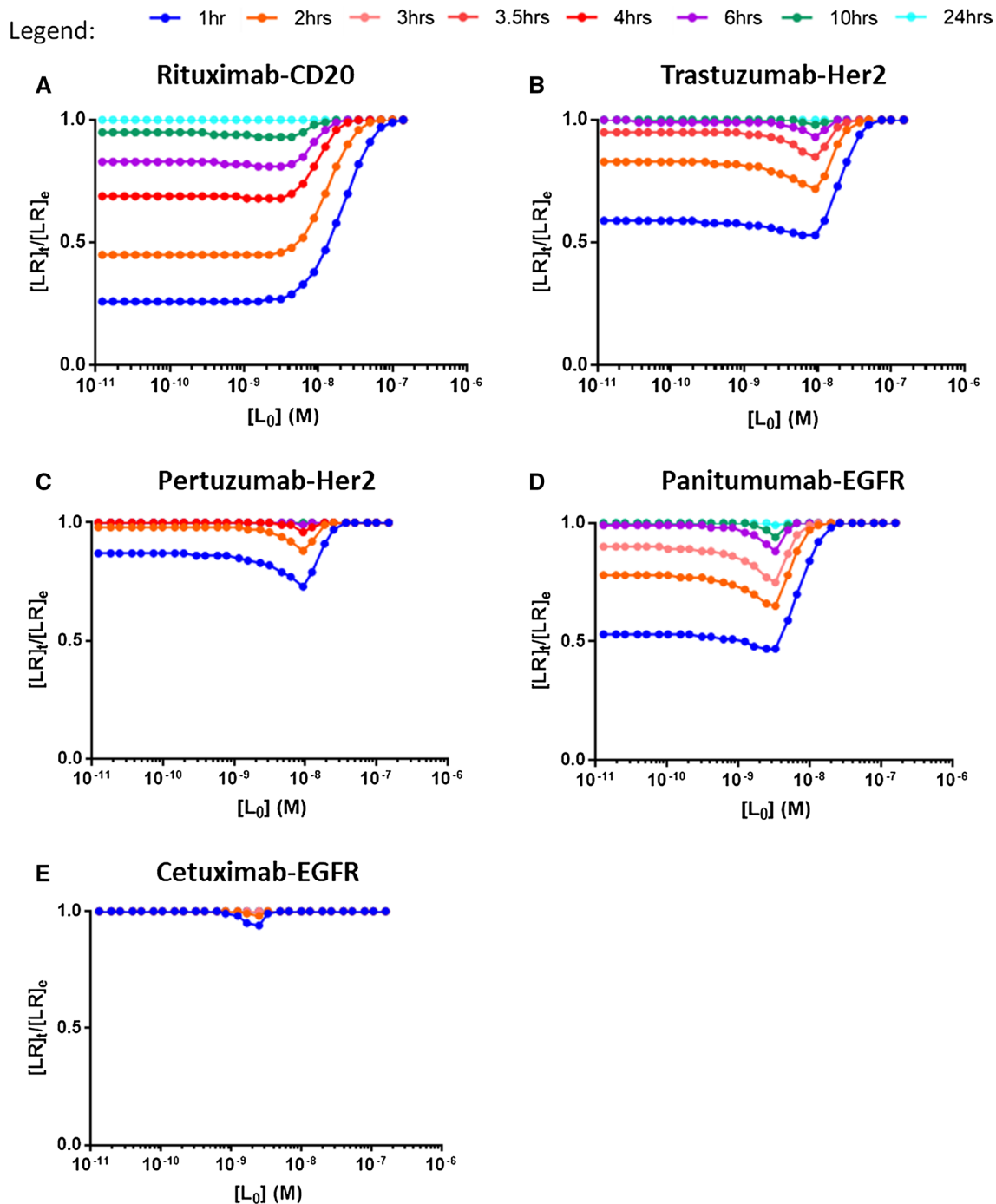


Fig. 5 Equilibrium charts for the studied systems based on binding kinetics obtained from LigandTracer data and receptor concentrations obtained from flow cytometry data (all systems except Panitumumab) or literature (Panitumumab). The ratio of the concentration

of the antibody–receptor complex at a given time ($[LR]_t$, from Eq. 3) and at time infinite ($[LR]_e$, from Eq. 5) was plotted against antibody concentration. At equilibrium, $[LR]_t = [LR]_e$ and the $[LR]_t/[LR]_e$ ratio is equal to 1

e.g., in the form of saturation binding curves, superimpose. It is important to appreciate, however, that when $R_0 > K_D$ only a small fraction of the curve (corresponding to a narrow range of low ligand concentrations near the saturation plateau phase—see below) contributes to the numerical

determination of K_D . For that narrow range of concentration, equilibration will take longer than for most of the rest of the data sets and it is, therefore, easy to wrongly consider that the system is at equilibrium, while it is not, and, furthermore, for the most important part of the curve (see Fig. 3).

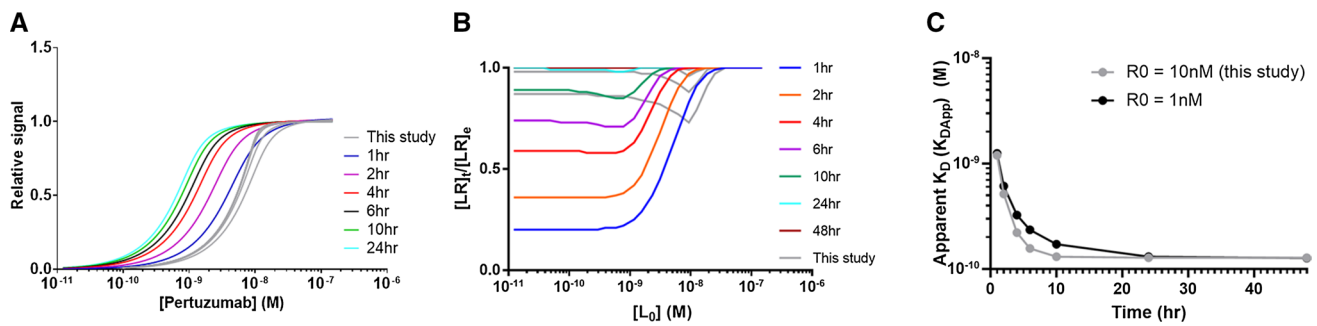


Fig. 6 Influence of receptor concentration R_0 on time to equilibrium and subsequent impact on K_{DApp} values exemplified by the Pertuzumab–HER2 system. A value of $R_0 = 1$ nM was compared with actual R_0 value (10 nM) used for experimental work in this study (light gray curves). **A** Simulated flow cytometry data (signal vs.

antibody concentration for various incubation times). **B** Degree of advancement of the reaction towards equilibrium ($[LR]/[LR]_e$ versus antibody concentration $[L_0]$). **C** Apparent K_D (K_{DApp}) vs. time of incubation

This can be illustrated here from the Trastuzumab–HER2, Pertuzumab–HER2, and Cetuximab–EGFR flow cytometry data which, from a rough visual examination, seemingly appeared close to the equilibrium after incubation times of 3.5, 2 and 2 h, respectively. Yet, K_{DApp} values obtained from fitting the curves with Eq. 6 differed significantly from the real K_D values (Fig. 4).

To explore this aspect further, we modeled, assuming unchanged kinetics, the Pertuzumab–HER2 interaction in an altered yet realistic setting, with $R_0 = 1$ nM (vs. 10 nM), which could for example be achieved using a low concentration of BT474 cells which express less HER2 receptors than SKOV3. The data are reported in Fig. 6, with predicted flow cytometry traces, time to equilibrium data, and subsequent effects on K_{DApp} values compared to the setting used in this paper. Despite a marked difference in the predicted time to equilibrium (reached only after 24–48 h compared to 4–6 h for the current setting with SKOV3 cells), the difference in K_{DApp} for each given incubation time is minimum between the two conditions, as shown in Fig. 6A–C, illustrating the fact that attempts to reach the equilibrium faster by increasing R_0 does not improve the robustness of affinity measurements on live cells.

It can also be appreciated from Fig. 6A that the shape of the curve changes significantly when increasing R_0 from 1 to 10 nM, resulting in the fact that for the higher R_0 value only a small part of the experimental data set, corresponding to the very top of the sigmoid curve, i.e., when a significant fraction of the receptor has been titrated, can be exploited to extract the value of K_D . In practice, any experimental variability in that part of the curve will thus have strong repercussions on the computed K_D value. The Cetuximab–EGFR interaction studied here is an extreme example of an R_0 -driven system, i.e., of a system not allowing K_D determination from equilibrium experiments,

because it is studied under conditions where R_0 is much larger than K_D .

Our recommendation to combine LigandTracer kinetic data with flow cytometry data, making no assumption on whether flow cytometry data are obtained at equilibrium or not, i.e., analyzing data with Eq. 4, eliminates all the risks described above and ensures robust determination of all the parameters describing the studied system, namely, k_{on} , k_{off} , K_D , and R_0 , even under conditions where R_0 is much larger than K_D .

Finally, for researchers wishing to analyze flow cytometry data only under equilibrium conditions, the knowledge of the kinetic constants obtained from LigandTracer experiments will allow said researchers to determine, as shown here from $[LR]/[LR]_e$ versus L_0 plots, the degree of completion of the reaction for any ligand concentration, and therefore, gain confidence that the experiment is conducted under proper conditions.

Conclusion

Screening for biologics has evolved significantly in the past decades and often involves live cell receptors as some categories of targets can be difficult to express as recombinant proteins. Furthermore, new generation biologics frequently present very high affinities towards their cognate receptors which represents new challenges. LigandTracer measures the equilibrium dissociation constant K_D from the ratio of binding kinetics, thereby bypassing the need to reach equilibrium. It can also record dissociation for hours and measure off rates slower than 10^{-5} s^{-1} , which are getting more frequent within this category of therapeutics. Finally, the technology uses live cells expressing functional receptors closer to in vivo conditions.

Flow cytometry measurements also involve live cells and titration with a labelled ligand to record molecular complex formation. However, measured K_D values do not always agree among those platforms. We hypothesized that these discrepancies, when they exist, originate most frequently from either flow cytometry experiments being recorded prior to full equilibration of the system or under conditions, where the receptor concentration is much larger than the value of the dissociation constant. Being operated under similar conditions, flow cytometry and LigandTracer platforms are thus ideal for cross-validation.

Ultimately, the goal of the drug discovery pipeline is to develop and produce safe and effective drugs. It is, therefore, essential to translate *in vitro* therapeutics–receptor interaction data in general, and K_D in particular, into hypothesis of biological effects. *In vitro* platforms are evolving, aiming to predict *in vivo* outcome such as described by Spiegelberg et al. (2016). Furthermore, joint analysis of binding kinetics, pharmacokinetics, target information, and dosage regimen during pharmacokinetic/pharmacodynamic modeling could be beneficial to early drug development (Georgi et al. 2018; Zhao and Schuck 2015). LigandTracer belongs to the arsenal of new tools now at the disposal of scientists to achieve these objectives.

Open Access This article is licensed under a Creative Commons Attribution 4.0 International License, which permits use, sharing, adaptation, distribution and reproduction in any medium or format, as long as you give appropriate credit to the original author(s) and the source, provide a link to the Creative Commons licence, and indicate if changes were made. The images or other third party material in this article are included in the article's Creative Commons licence, unless indicated otherwise in a credit line to the material. If material is not included in the article's Creative Commons licence and your intended use is not permitted by statutory regulation or exceeds the permitted use, you will need to obtain permission directly from the copyright holder. To view a copy of this licence, visit <http://creativecommons.org/licenses/by/4.0/>.

References

- Andersson K, Karlsson R, Löfås S, Franklin G, Hämäläinen MD (2006) Label-free kinetic binding data as a decisive element in drug discovery. *Expert Opin Drug Discov* 1:439–446
- Andersson K, Bjorkelund H, Malmqvist M (2010) Antibody–antigen interactions: what is the required time to equilibrium? *Nat Prec*. <https://doi.org/10.1038/npre.2010.5218.1>
- Barta P, Bjorkelund H, Andersson K (2011) Circumventing the requirement of binding saturation for receptor quantification using interaction kinetic extrapolation. *Nucl Med Commun* 32:863–867
- Barta P, Andersson K, Trejtnar F, Buijs J (2014) Exploring time-resolved characterization of the heterogeneity and dynamics of ligand–receptor interactions on living cells. *J Anal Oncol* 3:94–104
- Bjorkelund H, Andersson K (2006) Automated, high-resolution cellular retention and uptake studies *in vitro*. *Appl Radiat Isotopes* 64:901–905
- Bjorkelund H, Gedda L, Andersson K (2011) Comparing the epidermal growth factor interaction with four different cell lines: intriguing effects imply strong dependency of cellular context. *PLoS ONE* 6:e16536
- Bondza S, Foy E, Brooks J, Andersson K, Robinson J, Richalet P et al (2017) Real-time characterization of antibody binding to receptors on living immune cells. *Front Immunol* 8:455
- Bondza S, ten Broeke T, Nestor M, Leusen JHW, Buijs J (2020) Bivalent binding on cells varies between anti-CD20 antibodies and is dose-dependent. *Mabs* 12:1792673. <https://doi.org/10.1080/19420862.2020.1792673>
- Cacace A, Banks M, Spicer T, Civoli F, Watson J (2003) An ultra-HTS process for the identification of small molecule modulators of orphan G-protein-coupled receptors. *Drug Discov Today* 8:785–792
- Canziani GA, Klakamp S, Myszka DG (2004) Kinetic screening of antibodies from crude hybridoma samples using Biacore. *Anal Biochem* 325:301–307
- Cariuk P, Gardener MJ, Vaughan TJ (2013) Evolution of biologics screening technologies. *Pharmaceuticals (basel)* 6:681–688
- Copeland RA, Pompliano DL, Meek TD (2006) Drug–target residence time and its implications for lead optimization. *Nat Rev Drug Discov* 5:730–739
- Dahl G, Akerud T (2013) Pharmacokinetics and the drug–target residence time concept. *Drug Discov Today* 18:697–707
- Drake AW, Klakamp SL (2007) A rigorous multiple independent binding site model for determining cell-based equilibrium dissociation constants. *J Immunol Methods* 318:147–152
- Drake AW, Abdiche YN, Papalia GA (2018) Biophysical considerations for development of antibody-based therapeutics. In: Tabrizi M, Bornstein G, Klakamp S. Adis (eds) *Development of antibody-based therapeutics*, Singapore, pp 71–132
- Dubois L, Andersson K, Asplund A, Bjorkelund H (2013) Evaluating real-time immunohistochemistry on multiple tissue samples, multiple targets and multiple antibody labeling methods. *BMC Res Notes* 6:542
- Freeman DJ, McDorman K, Ogbagabriel S, Kozlosky C, Yang BB, Doshi S et al (2012) Tumor penetration and epidermal growth factor receptor saturation by panitumumab correlate with anti-tumor activity in a preclinical model of human cancer. *Mol Cancer* 11:47
- Georgi V, Schiele F, Berger BT, Steffen A, Marin Zapata PA, Briem H et al (2018) Binding kinetics survey of the drugged kinome. *J Am Chem Soc* 140:15774–15782
- Graff CP, Witttrup KD (2003) Theoretical analysis of antibody targeting of tumor spheroids: importance of dosage for penetration, and affinity for retention. *Cancer Res* 63:1288–1296
- Hulme EC, Trevethick MA (2010) Ligand binding assays at equilibrium validation and interpretation. *Br J Pharmacol* 161:1219–1237
- Jonsson A, Dogan J, Herne N, Abrahmsen L, Nygren PA (2008) Engineering of a femtomolar affinity binding protein to human serum albumin. *Protein Eng Des Sel* 21:515–527
- Morton TA, Myszka DG, Chaiken IM (1995) Interpreting complex binding kinetics from optical biosensors: a comparison of analysis by linearization, the integrated rate equation, and numerical integration. *Anal Biochem* 227:176–185
- Nilvebrant J, Kuku G, Bjorkelund H, Nestor M (2012) Selection and *in vitro* characterization of human CD44v6-binding antibody fragments. *Biotechnol Appl Biochem* 59:367–380
- Onell A, Andersson K (2005) Kinetic determinations of molecular interactions using Biacore–minimum data requirements for efficient experimental design. *J Mol Recognit* 18:307–317
- Pan AC, Borhani DW, Dror RO, Shaw DE (2013) Molecular determinants of drug–receptor binding kinetics. *Drug Discov Today* 18:667–673

- Pollard TD (2010) A guide to simple and informative binding assays. *Mol Biol Cell* 21:4061–4067
- Ram S, Kim D, Ober RJ, Ward ES (2014) The level of HER2 expression is a predictor of antibody-HER2 trafficking behavior in cancer cells. *Mabs* 6:1211–1219
- Rathanaswami P, Roalstad S, Roskos L, Su QJ, Lackie S, Babcook J (2005) Demonstration of an *in vivo* generated sub-picomolar affinity fully human monoclonal antibody to interleukin-8. *Biochem Bioph Res Co* 334:1004–1013
- Rathanaswami P, Babcook J, Gallo M (2008) High-affinity binding measurements of antibodies to cell-surface-expressed antigens. *Anal Biochem* 373:52–60
- Renaud JP, Chung CW, Danielson UH, Egner U, Hennig M, Hubbard RE et al (2016) Biophysics in drug discovery: impact, challenges and opportunities. *Nat Rev Drug Discov* 15:679–698
- Rich RL, Myszkowski DG (2009) Grading the commercial optical biosensor literature—Class of 2008: “The mighty binders.” *J Mol Recognit* 23:1–64
- Santiveri CM, López-Méndez B, Huecas S, Alfonso C, Luque-Ortega JR, Campos-Olivas R (2017). A Biophysical Toolkit for Molecular Interactions. <https://doi.org/10.1002/9780470015902.a0027015>
- Schreiber G (2002) Kinetic studies of protein–protein interactions. *Curr Opin Struct Biol* 12:41–47
- Selzer T, Albeck S, Schreiber G (2000) Rational design of faster associating and tighter binding protein complexes. *Nat Struct Biol* 7:537–541
- Spiegelberg D, Stenberg J, Haylock A-K, Nestor M (2016) A real-time *in vitro* assay as a potential predictor of *in vivo* tumor imaging properties. *Nucl Med Biol* 43:12–18
- Swinney DC (2008) Applications of binding kinetics to drug discovery, translation of binding mechanisms to clinically differentiated therapeutic responses. *Pharm Med* 22:23–34
- Swinney DC (2009) The role of binding kinetics in therapeutically useful drug action. *Curr Opin Drug Discov Devel* 12:31–39
- Tamaskovic R, Simon M, Stefan N, Schwill M, Pluckthun A (2012) Designed ankyrin repeat proteins (DARPs) from research to therapy. *Method Enzymol* 503:101–134
- Vaish A, Lin JS, McBride HJ, Grandsard PJ, Chen Q (2020) Binding affinity determination of therapeutic antibodies to membrane protein targets: kinetic exclusion assay using cellular membranes for anti-CD20 antibody. *Anal Biochem* 609:113974. <https://doi.org/10.1016/j.ab.2020.113974>
- Vanhove E, Vanhove M (2018) Affinity determination of biomolecules: a kinetic model for the analysis of pre-equilibrium titration curves. *Eur Biophys J* 47:961–966
- Wood ER, Truesdale AT, McDonald OB, Yuan D, Hassell A, Dickerson SH et al (2004) A unique structure for epidermal growth factor receptor bound to GW572016 (Lapatinib): relationships among protein conformation, inhibitor off-rate, and receptor activity in tumor cells. *Cancer Res* 64:6652–6659
- Zhao H, Schuck P (2015) Combining biophysical methods for the analysis of protein complex stoichiometry and affinity in SEDPHAT. *Acta Crystallogr D Biol Crystallogr* 71:3–14

Publisher's Note Springer Nature remains neutral with regard to jurisdictional claims in published maps and institutional affiliations.